

# Catalytic asymmetric C–N cross-coupling towards boron-stereogenic 3-amino-BODIPYs

Received: 23 June 2024

Accepted: 23 December 2024

Published online: 07 January 2025

Check for updates

Baoquan Zhan<sup>1,2,3</sup>, Li-Qing Ren<sup>2,3</sup>, Jiayi Zhao<sup>2</sup>, Hua Zhang<sup>1</sup>✉ & Chuan He<sup>2</sup>✉

3-Amino boron dipyrromethenes (BODIPYs) are a versatile class of fluorophores widely utilized in live cell imaging, photodynamic therapy, and fluorescent materials science. Despite the growing demand for optically active BODIPYs, the synthesis of chiral 3-amino-BODIPYs, particularly the catalytic asymmetric version, remains a challenge. Herein, we report the synthesis of boron-stereogenic 3-amino-BODIPYs via a palladium-catalyzed desymmetric C–N cross-coupling of prochiral 3,5-dihalogen-BODIPYs. This approach features a broad substrate scope, excellent functional group tolerance, high efficiency, and remarkable enantioselectivities, under mild reaction conditions. Further stereospecific formation of chiral 3,5-diamino-BODIPYs, along with an investigation into the photophysical properties of the resulting optical BODIPYs are also explored. This asymmetric protocol not only enriches the chemical space of chiroptical BODIPY dyes but also contributes to the realm of chiral boron chemistry.

Boron dipyrromethenes (BODIPYs) are one of the most efficient classes of fluorophores, renowned for their exceptional spectroscopic and photophysical properties<sup>1–5</sup>. Their versatility has led to widespread applications across various fields, including biology<sup>6–11</sup>, pharmaceuticals<sup>12–16</sup>, and materials science<sup>17–25</sup>. Of particular interest is the incorporation of an amine substituent at the  $\alpha$  position of BODIPY, giving rise to 3-amino-BODIPYs, which have garnered significant attention. These compounds have found extensive utility as fluorescent sensors and probes for biological imaging and labeling<sup>26–37</sup>, as well as in the development of endoplasmic reticulum-targeting reagents<sup>38</sup> and high-performance narrowband red OLEDs<sup>39</sup> (Fig. 1a). However, despite the increasing demand for chiroptical luminophores capable of chiral sensing and labeling<sup>40–51</sup>, exploration of chiral 3-amino-BODIPYs has remained limited, with existing studies primarily focusing on chirality at the periphery of the BODIPY core<sup>52–56</sup>. To date, the synthesis of boron-stereogenic 3-amino-BODIPYs has remained

unexplored (Fig. 1a). Notably, the construction of boron-stereogenic chirality in a catalytic asymmetric manner has seen limited success until recently due to the lack of effective synthetic tools and the potential instability of ligands attached to the boron atom<sup>57–60</sup>. Given their significant importance and vast potential applications, the development of efficient catalytic asymmetric methods for constructing enantioenriched boron-stereogenic 3-amino-BODIPYs emerges as an enticing and highly desirable objective.

From a retrosynthetic analysis, we devised a synthetic strategy for boron-stereogenic 3-amino-BODIPYs by employing a desymmetric C–N cross-coupling approach starting from prochiral 3,5-dihalogen-BODIPYs (Fig. 1b). In recent years, catalytic asymmetric C–N cross-coupling has emerged as a powerful tool for constructing various amine compounds featuring centered, axial, and planar chirality<sup>61–66</sup>. However, due to the unique reactivity of 3,5-dihalogen-BODIPYs, several side-reactions may occur when attempting the desymmetric C–N

<sup>1</sup>Key Laboratory of Catalysis and Energy Materials Chemistry of Ministry of Education, Hubei Key Laboratory of Catalysis and Materials Science, School of Chemistry and Materials Science, South-Central Minzu University, Wuhan, Hubei, China. <sup>2</sup>Shenzhen Grubbs Institute and Department of Chemistry, Shenzhen Key Laboratory of Small Molecule Drug Discovery and Synthesis, Guangdong Provincial Key Laboratory of Catalysis, Southern University of Science and Technology, Shenzhen, Guangdong, China. <sup>3</sup>These authors contributed equally: Baoquan Zhan, Li-Qing Ren. ✉e-mail: [huazhang@scuec.edu.cn](mailto:huazhang@scuec.edu.cn); [hec@sustech.edu.cn](mailto:hec@sustech.edu.cn)

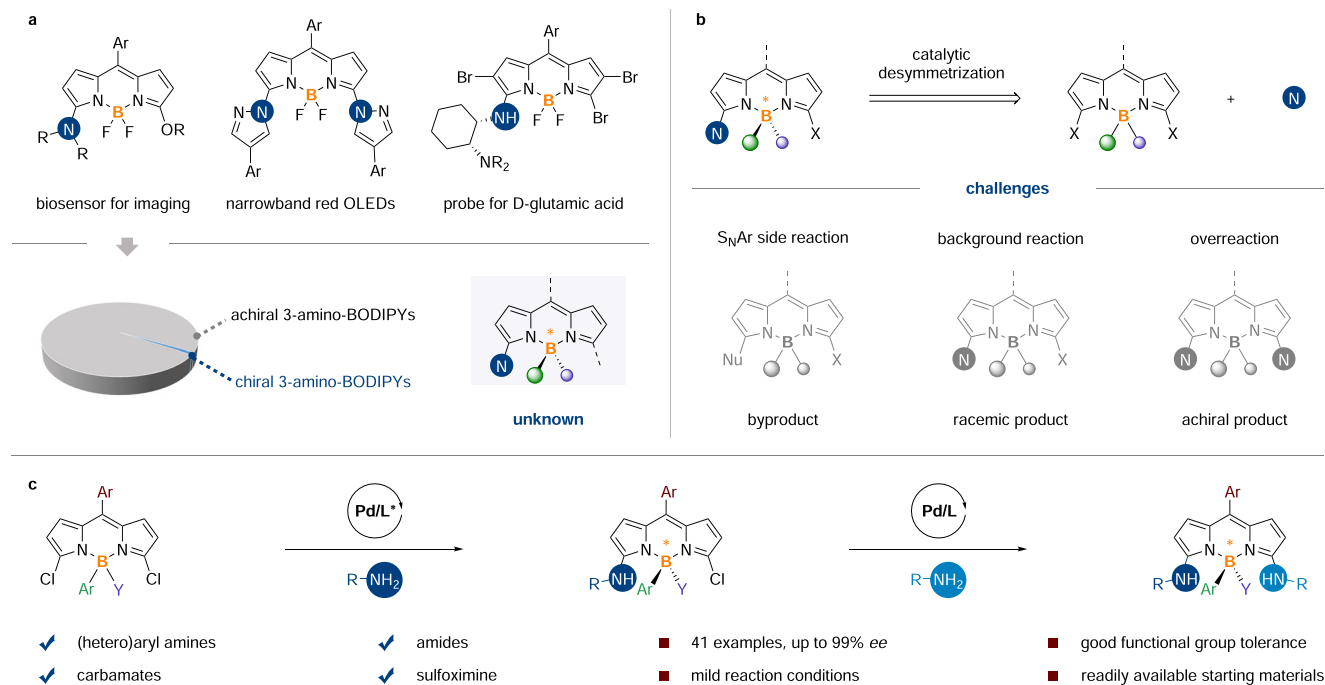


**Fig. 1 | Importance and synthesis of boron-stereogenic 3-amino-BODIPYs. a** Selected 3-amino-BODIPYs with important applications. **b** Design plan and challenges towards boron-stereogenic 3-amino-BODIPYs. **c** Catalytic asymmetric synthesis of boron-stereogenic 3-amino-BODIPYs (this work).

cross-coupling: (1)  $S_NAr$  reaction of 3,5-dihalogen-BODIPYs with strong nucleophilic reagents such as alkoxy bases<sup>67</sup>; (2) direct background reaction of 3,5-dihalogen-BODIPYs with amines, leading to racemic products<sup>68,69</sup>; (3) overreaction resulting in the formation of achiral 3,5-diamino-BODIPYs<sup>70</sup>. Therefore, the selection of an efficient asymmetric catalytic system is crucial for the success of the desired enantioselective transformation. In this study, we report a convenient approach for the synthesis of boron-stereogenic 3-amino-BODIPYs via a palladium-catalyzed asymmetric C–N cross-coupling (Fig. 1c). This transformation features a broad substrate scope, high compatibility with functional groups, and excellent enantioselectivity. In addition, derivatizations and photophysical properties of the obtained chiral 3-amino-BODIPYs are also investigated to illustrate the utility of this asymmetric protocol.

## Results and discussion

### Reaction development

Our study commenced with the evaluation of the C–N cross-coupling between prochiral 3,5-dichlorinated BODIPY (**1a**) and *p*-toluidine (**2a**). After numerous trials and careful analysis, we found that the occurrence of  $S_NAr$  side reaction and overreaction could be circumvented by employing a non-nucleophilic base such as  $Cs_2CO_3$  under mild conditions. In addition, the background reaction occurred in the absence of a catalyst giving the racemic **3a** in an 85% yield after 12 h (Table 1, entry 1). Encouragingly, by shortening the reaction time to 2 h, the background reaction was significantly diminished (Table 1, entry 2), opening the possibility of achieving enantiocontrol when an effective chiral catalyst was employed. Initial attempts using  $Pd(dba)_2$  (4 mol%) as the catalyst precursor and *R*-BINAP (**L1**) (10 mol%) as the ligand, in the presence of  $Cs_2CO_3$  (2.0 equiv) in toluene at 60 °C, the target boron-stereogenic 3-amino-BODIPY **3a** could be obtained in a 29% yield with 18% *ee* (enantiomeric excess) (Table 1, entry 3). To assess the impact of different ligands on this asymmetric C–N cross-coupling reaction, a variety of chiral phosphine ligands were examined. The use of electron-rich bidentate phosphine ligands such as Segphos (**L2**) and Josiphos (**L3**) provided similar yields but lower enantioselectivities (Table 1, entries 4 and 5). Employing an electron-rich monodentate phosphine ligand,

MeO-MOP (**L4**), yielded a high yield of **3a** but low enantioselectivity (Table 1, entry 6). Then, various electron-deficient chiral ligands including TADDOL-derived phosphoramidite (**L5**) and BINOL-derived phosphoramidites (**L6–L9**) were further evaluated (Table 1, entries 7–11). The results demonstrated a correlation between increased enantioselectivity and enhanced steric hindrance of the chiral ligand. In this way, we finally established the optimal conditions wherein **3a** was obtained in a 99% yield with 98% *ee* within 2 h using phosphoramidite **L9** as the ligand (Table 1, entry 11). Notably, the use of a phosphoramidite ligand without axial chirality (**L10**) resulted in lower enantioselectivity (Table 1, entry 12). When  $K_2CO_3$  was used instead of  $Cs_2CO_3$ , both yield and *ee* were reduced dramatically (Table 1, entry 13). The use of THF as the solvent led to a similar yield of **3a** with lower enantioselectivity, while lowering the temperature to room temperature resulted in a trace amount of **3a** (Table 1, entries 14 and 15).

### Substrate scope

Having established the optimal reaction conditions, we proceeded to investigate the scope of amines in the catalytic asymmetric C–N cross-coupling reaction and the results are summarized in Fig. 2. In general, both electron-donating and electron-withdrawing substituents at the ortho, meta, or para positions of anilines were well accommodated in this transformation. Anilines with electron-donating substituents, such as methyl, methoxy, and diphenylamino groups (**3a**, **3c**, **3d**, **3j**, **3l**), underwent smooth asymmetric C–N cross-coupling, affording the desired products in excellent yields with high enantioselectivities. Similarly, anilines with electron-withdrawing substituents, including ester, trifluoromethyl, and cyano groups (**3e**, **3g**, **3k**), were compatible with this asymmetric C–N cross-coupling and successfully delivered the desired products in excellent yields with high enantioselectivities. Remarkably, susceptible substituents such as alkynyl (**3h**) and hydroxymethyl groups (**3i**), as well as halogen substituents such as chloride (**3n**, **3x**) and bromide (**3f**, **3m**, **3o**, **3p**), were all well-tolerated in this transformation, making further downstream functionalization feasible. Furthermore, anilines bearing multiple substituents exhibited good compatibility in this asymmetric cross-coupling reaction (**3n**–**3p**). The absolute configuration of the enantioenriched **3o** was

**Table 1 | Optimization of the reaction conditions.<sup>a</sup>**

Reaction scheme: **1a** + **2a** (Tol-NH<sub>2</sub>) → **3a** (Pd(dba)<sub>2</sub> (4 mol%), L (10 mol%), base (2.0 equiv), solvent, 60 °C, time)

Chemical structures of ligands L1-L10 are shown below the reaction scheme.

Entry	[Pd]/L	Time	Base	Solvent	Yield of <b>3a</b> (%)	ee of <b>3a</b> (%)
1	-	12 h	Cs <sub>2</sub> CO <sub>3</sub>	toluene	85	-
2	-	2 h	Cs <sub>2</sub> CO <sub>3</sub>	toluene	6	-
3	Pd(dba) <sub>2</sub> /L1	2 h	Cs <sub>2</sub> CO <sub>3</sub>	toluene	29	18
4	Pd(dba) <sub>2</sub> /L2	2 h	Cs <sub>2</sub> CO <sub>3</sub>	toluene	20	2
5	Pd(dba) <sub>2</sub> /L3	2 h	Cs <sub>2</sub> CO <sub>3</sub>	toluene	25	6
6	Pd(dba) <sub>2</sub> /L4	2 h	Cs <sub>2</sub> CO <sub>3</sub>	toluene	94	22
7	Pd(dba) <sub>2</sub> /L5	2 h	Cs <sub>2</sub> CO <sub>3</sub>	toluene	74	44
8	Pd(dba) <sub>2</sub> /L6	2 h	Cs <sub>2</sub> CO <sub>3</sub>	toluene	37	40
9	Pd(dba) <sub>2</sub> /L7	2 h	Cs <sub>2</sub> CO <sub>3</sub>	toluene	91	72
10	Pd(dba) <sub>2</sub> /L8	2 h	Cs <sub>2</sub> CO <sub>3</sub>	toluene	70	89
11	Pd(dba) <sub>2</sub> /L9	2 h	Cs <sub>2</sub> CO <sub>3</sub>	toluene	99	98
12	Pd(dba) <sub>2</sub> /L10	2 h	Cs <sub>2</sub> CO <sub>3</sub>	toluene	97	58
13	Pd(dba) <sub>2</sub> /L9	2 h	K <sub>2</sub> CO <sub>3</sub>	toluene	12	16
14	Pd(dba) <sub>2</sub> /L9	2 h	Cs <sub>2</sub> CO <sub>3</sub>	THF	99	74
15 <sup>b</sup>	Pd(dba) <sub>2</sub> /L9	2 h	Cs <sub>2</sub> CO <sub>3</sub>	toluene	4	-

<sup>a</sup>Standard conditions: **1a** (0.1 mmol), **2a** (0.1 mmol), Pd(dba)<sub>2</sub> (4 mol%), L (10 mol%), base (2.0 equiv), in 1.0 mL of solvent under argon atmosphere at 60 °C. The yield was determined by <sup>1</sup>H NMR using 1,1,2,2-tetrachloroethane as the internal standard. The ee values were determined by chiral HPLC; <sup>b</sup>Reaction at room temperature for 2 h. Ph, phenyl; Tol, *p*-tolyl.

determined through X-ray crystallographic analysis (CCDC 2323832). Additionally, aromatic amines with fused aromatic cores (e.g., naphthalene and pyrene) and heteroaromatic cores (e.g., benzodioxole, benzothiofene, indole, carbazole, quinoline, and pyrimidine) proved to be successful substrates (**3q–3x**). Moreover, this catalytic asymmetric C–N cross-coupling was also applicable to amides. Both alkylamides and aryl-amides underwent smooth asymmetric C–N cross-coupling, yielding the corresponding products in moderate to good yields with good to excellent enantioselectivities (**3y–3aa**). Notably, the reaction of N-Boc and N-Cbz amides produced the desired chiral 3-amino-BODIPYs in 88 and 92% yield with 98% ee, respectively (**3ab**, **3ac**). To our delight, sulfoximine **2ad** was also a suitable substrate for this reaction, delivering the corresponding product **3ad** in excellent result (91% yield, >99% ee). In addition, an interesting 1,4-bisphenylene-diamine-bridged BODIPY dimer **3ae** was also assembled in a smooth manner with 63% yield and 99% ee. Several unsuccessful amine examples are shown in Fig. S1.

After evaluating the scope of amines, we then assessed the generality of this process concerning the BODIPY scaffold (Fig. 3). The catalytic asymmetric C–N cross-coupling of BODIPYs bearing various aryl substituents at the meso position proceeded smoothly, providing the corresponding boron-stereogenic 3-amino-BODIPYs in good yields with high enantioselectivities (**4a–4d**). It is worth mentioning that, this C–N cross-coupling occurred chemoselectively, leaving the aromatic C–Cl bond in the meso aryl substituent intact (**4b**). Notably, the

substituents on the boron atom of the BODIPY framework were not limited to phenyl and fluorine. Substituents on boron with diverse steric and electronic effects, including naphthyl, 4-fluorophenyl, thieryl, and methyl groups, were well tolerated, leading to the desired products in good to excellent yields with excellent enantioselectivities (**4e**, **4f**, **4h**, **4i**). BODIPYs featuring methoxy and 4-cyanophenyl substituents on the boron atom exhibited slightly lower enantioselectivities (**4g**, **4j**).

To showcase the synthetic potential of this approach, a gram-scale experiment was carried out involving the reaction between **1a** and **2a**, which resulted in the desired product **3a** in a yield of 91% with 94% ee (Fig. 4). Furthermore, the remaining chlorine group in **3a** could be further converted into various amino groups, allowing access to chiral 3,5-diamino-BODIPYs in a stereospecific manner. In the presence of a Pd/Xphos catalytic system, the C–N cross-coupling of **3a** with diverse aromatic and aliphatic amines proceeded smoothly, affording the desired chiral 3,5-diamino-BODIPYs in moderate to good yields without the loss of ee (**5a–5f**). In addition to the C–N coupling reaction, the Suzuki cross-coupling reaction also proceeded smoothly, yielding the corresponding C–C cross-coupling products **5g** and **5h** in good yields without the loss of ee.

### Photophysical properties investigations

With a diverse array of enantioenriched boron-stereogenic 3-amino BODIPYs in hand, we proceeded to investigate the photophysical

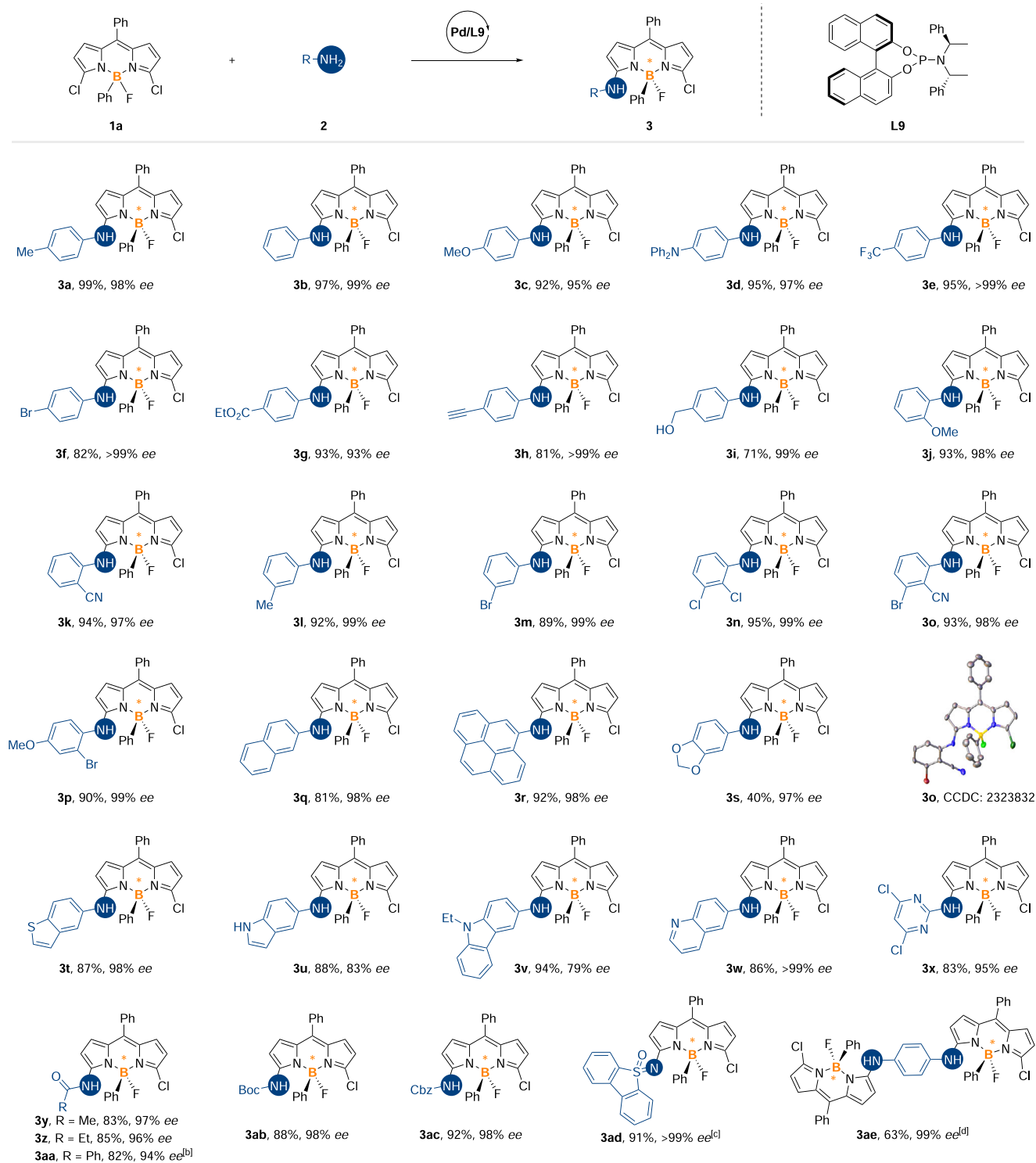


**Fig. 2 | Substrate scope for amines.** **a** Standard conditions: **1a** (0.1 mmol), **2** (0.1 mmol), Pd(dba)<sub>2</sub> (4 mol%), **L9** (10 mol%), Cs<sub>2</sub>CO<sub>3</sub> (2.0 equiv), in 1.0 mL of toluene under argon atmosphere at 60 °C for 2 h. Isolated yields. The ee values were determined by chiral HPLC; (**b**) 2.0 equiv of **2** was used. X-ray crystallographic

analysis determined that the absolute configuration of **3o** is (*R*). **c** 1.0 equiv of sulfoximine was used. **d** **1a** (0.2 mmol), **2** (0.1 mmol), a 25% yield of *meso* isomer was also detected (mixture). Ph phenyl, Boc *tert*-butoxycarbonyl, Cbz benzyloxycarbonyl.

properties of selected products (Fig. 5). In comparison to the 3-amino-BODIPYs (**3a**, **3r**, and **3y**), the 3,5-diamino-BODIPYs (**5c**, **5e**) exhibited a remarkable red shift in both absorption and emission maxima (Fig. 5a, b). Notably, compounds **3r**, **5c**, and **5h** displayed emission maxima in the first near-infrared region (NIR-I), rendering it potentially suitable for various applications such as labeling reagents, photodynamic therapy, and chemosensors. Additionally, the chiroptical properties of **3r**, **5g**, **5h**,

and their enantiomers were investigated using circular dichroism (CD) spectroscopies. The CD spectra exhibited mirror images of each other, demonstrating clear Cotton effects at approximately 512, 565 and 556 nm, respectively (Fig. 5c). To our delight, **5g** and **5h** also exhibited CPL activity from 500 to 750 nm, with  $|g_{lum}|$  up to  $2.6 \times 10^{-4}$  (634 nm) and  $4.5 \times 10^{-4}$  (648 nm), respectively (Fig. 5d). Moreover, we also investigated the fluorescence quantum yields and fluorescence lifetimes of

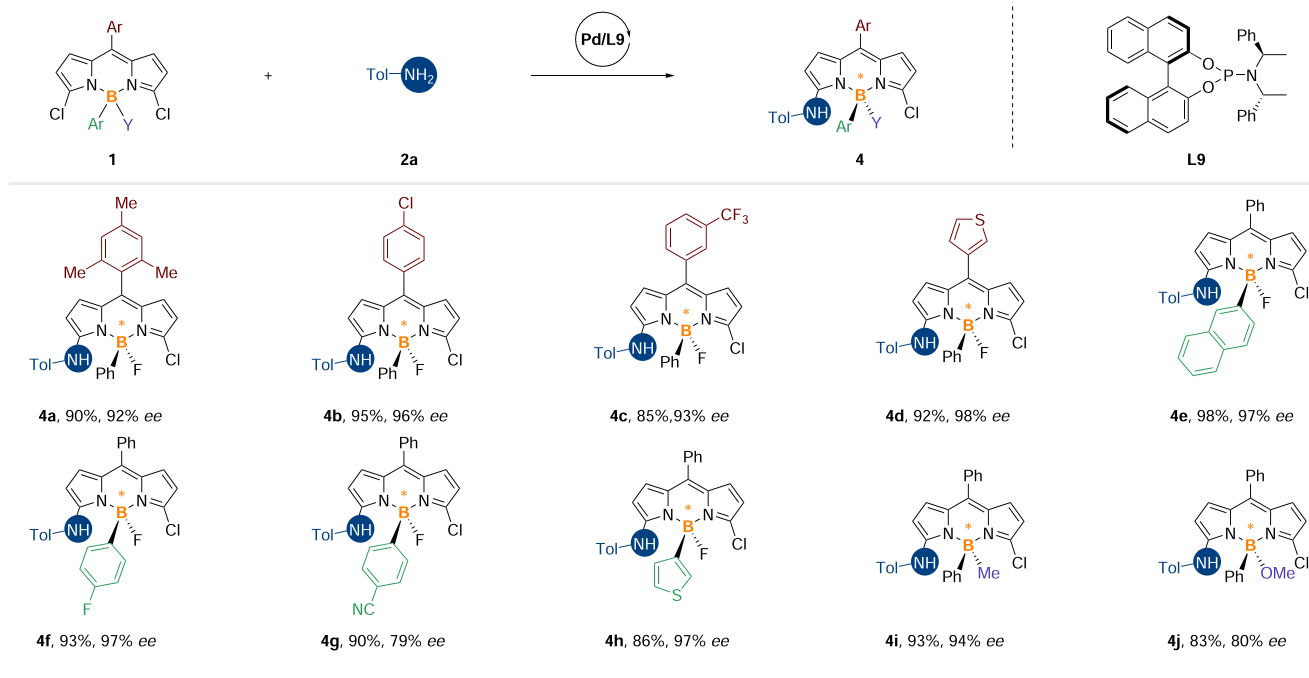


**Fig. 3 | Substrate scope for BODIPYs.** **a** Standard conditions: **1** (0.1 mmol), **2a** (0.1 mmol), Pd(dba)<sub>2</sub> (4 mol%), **L9** (10 mol%), Cs<sub>2</sub>CO<sub>3</sub> (2.0 equiv), in 1.0 mL of toluene under argon atmosphere at 60 °C for 2 h. Isolated yields. The ee values were determined by chiral HPLC. Ar aryl, Ph phenyl, Tol *p*-tolyl.

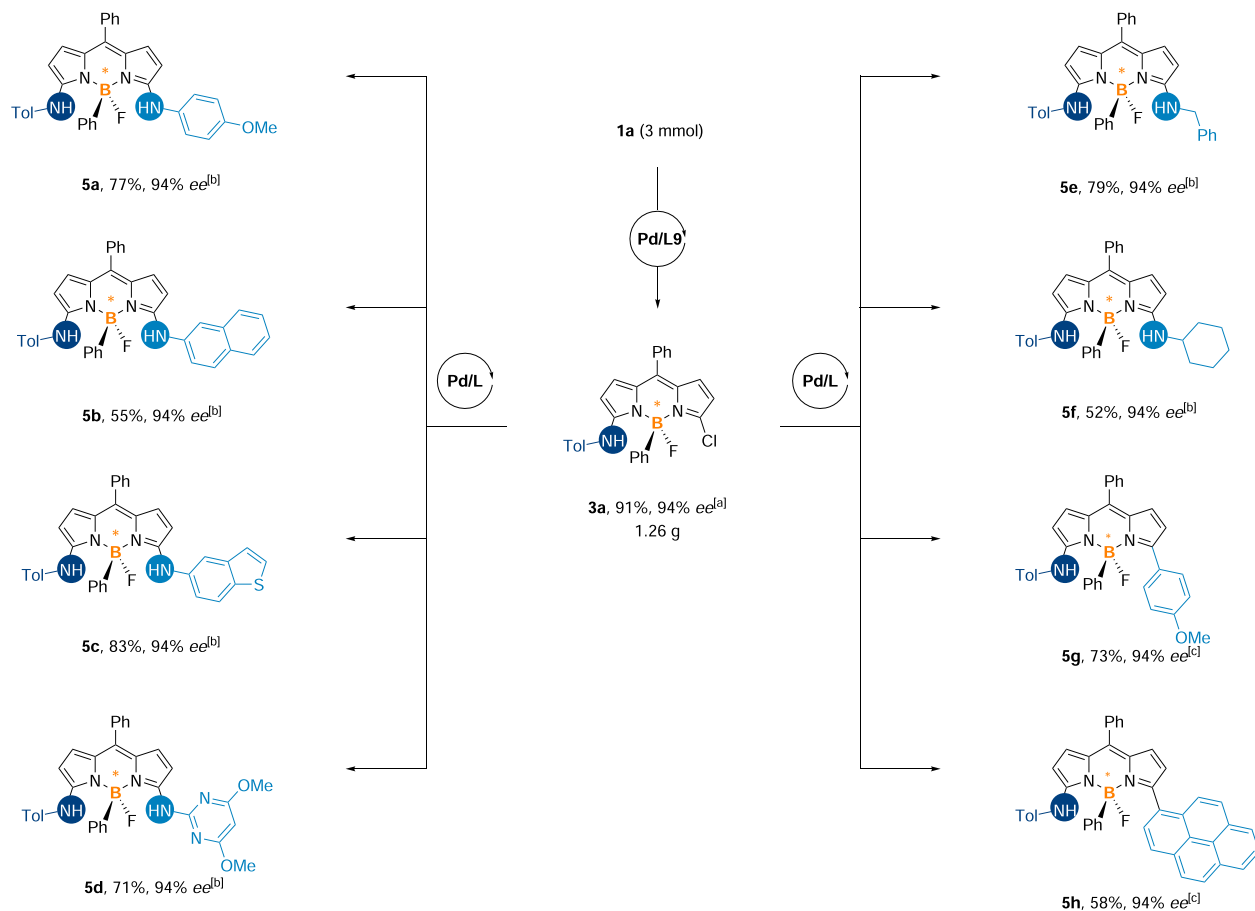


**Fig. 4 | Derivatization of boron-stereogenic 3-amino-BODIPYs.** **a** **1a** (3 mmol), **2a** (3 mmol), Pd(dba)<sub>2</sub> (2 mol%), **L9** (5 mol%), Cs<sub>2</sub>CO<sub>3</sub> (2.0 equiv), in 10 mL of toluene under argon atmosphere at 60 °C for 12 h. **b** **3a** (0.1 mmol), amine (2.0 equiv), Pd(OAc)<sub>2</sub> (10 mol%), Xphos (30 mol%), Cs<sub>2</sub>CO<sub>3</sub> (2.0 equiv), in 1.0 mL of toluene

under argon atmosphere at 100 °C for 4 h. **c** **3a** (0.1 mmol), arylboronic acid (1.0 equiv), Pd(OAc)<sub>2</sub> (10 mol%), Sphos (10 mol%), Et<sub>3</sub>N (2.0 equiv), in 1.0 mL of TBME (*t*-butyl methyl ether) under argon atmosphere at 80 °C for 24 h. Isolated yields. The ee values were determined by chiral HPLC. Ph phenyl, Tol *p*-tolyl.



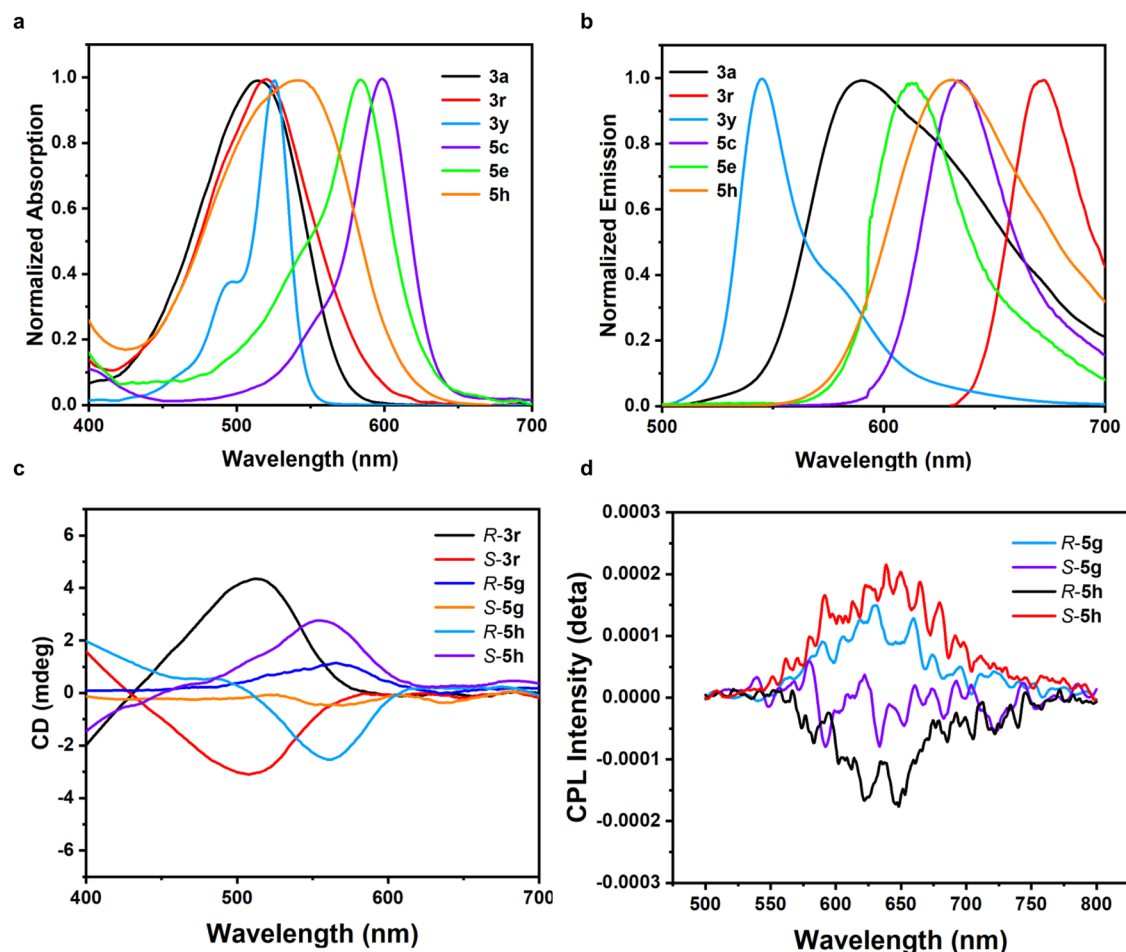


**Fig. 5 | Photophysical property investigations.** **a** Absorption spectra of **3a**, **3r**, **3y**, **5c**, **5e**, and **5h** in  $\text{CH}_2\text{Cl}_2$  ( $10^{-5}$  M). **b** Emission spectra of **3a**, **3r**, **3y**, **5c**, **5e**, and **5h** in  $\text{CH}_2\text{Cl}_2$  ( $10^{-5}$  M). **c** CD spectra of **3r**, **5g** and **5h** in  $\text{CH}_2\text{Cl}_2$  ( $10^{-5}$  M). **d** CPL spectra of **5g** and **5h** in  $\text{CH}_2\text{Cl}_2$  ( $2 \times 10^{-5}$  M).

several representative examples (Fig. S3). The 3,5-diamino-BODIPYs (**5c** and **5e**) exhibit higher fluorescence quantum yields than those of 3-amino-BODIPYs (**3a**, **3y**, **4h**, and **4i**). Compounds **4h**, **5c**, and **5e** showed longer fluorescence lifetimes ( $\geq 3.60$  ns). These characteristics expand the diversity of the chiroptical BODIPY dye platform, making it potentially appealing in the fields of biological, medicinal, and material chemistry as chiroptical luminophores.

In summary, we have developed a straightforward approach for achieving boron-stereogenic chirality through catalytic asymmetric C–N cross-coupling. This method enables the synthesis of a wide range of boron-stereogenic 3-amino-BODIPYs in decent yields with excellent enantioselectivities, which could be further converted to chiral 3,5-diamino-BODIPYs via a second stereospecific C–N cross-coupling. Additionally, we have investigated the photophysical properties of the obtained chiroptical BODIPYs. We believe this work not only enriches the chemical diversity of chiroptical BODIPY dyes but also inspires further advances in chiral boron chemistry.

## Methods

### General procedure for the enantioselective synthesis of boron-stereogenic BODIPY 3

Inside an argon-filled glovebox, an oven-dried 5 mL microwave reaction tube was charged with  $\text{Pd}(\text{dba})_2$  (2.2 mg, 0.004 mmol), **L9** (5.4 mg, 0.01 mmol), and anhydrous toluene (0.5 mL). After stirring for 5 min,  $\text{Cs}_2\text{CO}_3$  (65.2 mg, 0.2 mmol), **1a** (39.5 mg, 0.1 mmol), and primary amine (1.0 equiv to 2.0 equiv) were added, followed by the addition of toluene (0.5 mL). The tube was capped and taken outside of the glovebox. The resulting mixture was placed into a pre-heated (60 °C)

aluminum block and stirred for 2 h. Then the reaction mixture was concentrated and purified by column chromatography using preparative TLC (petroleum ether/ethyl acetate, from 10:1 to 3:1) as the eluent to afford the target product.

## Data availability

The data that support the findings of this study are available within the paper and its Supplementary Information. Data supporting the findings of this manuscript are also available from the corresponding author upon request. Details about materials and methods, experimental procedures, characterisation data,  $^1\text{H}$ ,  $^{13}\text{C}$ ,  $^{19}\text{F}$ ,  $^{11}\text{B}$  NMR spectra and mass spectrometry data are available in Supplementary Information. Crystallographic data for the structure reported in this Article have been deposited at the Cambridge Crystallographic Data Centre, under deposition number CCDC 2323832 (**3o**). Copies of the data can be obtained free of charge via <https://www.ccdc.cam.ac.uk/structures/>.

## References

- Loudet, A. & Burgess, K. BODIPY dyes and their derivatives: syntheses and spectroscopic properties. *Chem. Rev.* **107**, 4891–4932 (2007).
- Ulrich, G., Ziessel, R. & Harriman, A. The chemistry of fluorescent BODIPY dyes: versatility unsurpassed. *Angew. Chem. Int. Ed.* **47**, 1184–1201 (2008).
- Boens, N., Leen, V. & Dehaen, W. Fluorescent indicators based on BODIPY. *Chem. Soc. Rev.* **41**, 1130–1172 (2012).
- Lu, H., Mack, J., Yang, Y. & Shen, Z. Structural modification strategies for the rational design of red/NIR region BODIPYs. *Chem. Soc. Rev.* **43**, 4778–4823 (2014).

5. Bumagina, N. A. et al. Basic structural modifications for improving the practical properties of BODIPY. *Coord. Chem. Rev.* **469**, 214684 (2022).
6. Gonçalves, M. S. T. Fluorescent labeling of biomolecules with organic probes. *Chem. Rev.* **109**, 190–212 (2009).
7. Kowada, T., Maeda, H. & Kikuchi, K. BODIPY-based probes for the fluorescence imaging of biomolecules in living cells. *Chem. Soc. Rev.* **44**, 4953–4972 (2015).
8. Bertrand, B. et al. Metal-based BODIPY derivatives as multimodal tools for life sciences. *Coord. Chem. Rev.* **358**, 108–124 (2018).
9. Kolemen, S. & Akkaya, E. U. Reaction-based BODIPY probes for selective bio-imaging. *Coord. Chem. Rev.* **354**, 121–134 (2018).
10. Gai, L., Liu, Y., Zhou, Z., Lu, H. & Guo, Z. BODIPY-based probes for hypoxic environments. *Coord. Chem. Rev.* **481**, 215041 (2023).
11. Wang, S. et al. Mitochondria-targeted BODIPY dyes for small molecule recognition, bio-imaging and photodynamic therapy. *Chem. Soc. Rev.* **53**, 3976–4019 (2024).
12. Kamkaew, A. et al. BODIPY dyes in photodynamic therapy. *Chem. Soc. Rev.* **42**, 77–88 (2013).
13. Zhang, T., Ma, C., Sun, T. & Xie, Z. Unadulterated BODIPY nanoparticles for biomedical applications. *Coord. Chem. Rev.* **390**, 76–85 (2019).
14. Nguyen, V.-N. et al. Recent developments of BODIPY-based colorimetric and fluorescent probes for the detection of reactive oxygen/nitrogen species and cancer diagnosis. *Coord. Chem. Rev.* **439**, 213936 (2021).
15. Mao, Z. et al. Engineering of BODIPY-based theranostics for cancer therapy. *Coord. Chem. Rev.* **476**, 214908 (2023).
16. Wang, J., Gong, Q., Jiao, L. & Hao, E. Research advances in BODIPY-assembled supramolecular photosensitizers for photodynamic therapy. *Coord. Chem. Rev.* **496**, 215367 (2023).
17. Li, D., Zhang, H. & Wang, Y. Four-coordinate organoboron compounds for organic light-emitting diodes (OLEDs). *Chem. Soc. Rev.* **42**, 8416–8433 (2013).
18. Bessette, A. & Hanan, G. S. Design, synthesis and photophysical studies of dipyrromethene-based materials: insights into their applications in organic photovoltaic devices. *Chem. Soc. Rev.* **43**, 3342–3405 (2014).
19. Maeda, C., Nagahata, K., Shirakawa, T. & Ema, T. Azahelicene-fused BODIPY analogues showing circularly polarized luminescence. *Angew. Chem. Int. Ed.* **59**, 7813–7817 (2020).
20. Poddar, M. & Misra, R. Recent advances of BODIPY based derivatives for optoelectronic applications. *Coord. Chem. Rev.* **421**, 213462 (2020).
21. Li, F.-Z., Yin, J.-F. & Kuang, G.-C. BODIPY-based supramolecules: construction, properties and functions. *Coord. Chem. Rev.* **448**, 214157 (2021).
22. Gupta, G., Sun, Y., Das, A., Stang, P. J. & Yeon Lee, C. BODIPY based metal-organic macrocycles and frameworks: recent therapeutic developments. *Coord. Chem. Rev.* **452**, 214308 (2022).
23. Wang, J., Yu, C., Hao, E. & Jiao, L. Conformationally restricted and ring-fused aza-BODIPYs as promising near infrared absorbing and emitting dyes. *Coord. Chem. Rev.* **470**, 214709 (2022).
24. Wang, Y. et al. BODIPY-based supramolecular fluorescent metal-lacages. *Chin. Chem. Lett.* **34**, 107576 (2023).
25. Li, Y. et al. Near-infrared boron-dipyrin (BODIPY) nanomaterials: molecular design and anti-tumor therapeutics. *Coord. Chem. Rev.* **506**, 215718 (2024).
26. Domaille, D. W., Zeng, L. & Chang, C. J. Visualizing ascorbate-triggered release of labile copper within living cells using a ratiometric fluorescent sensor. *J. Am. Chem. Soc.* **132**, 1194–1195 (2010).
27. Dodani, S. C., Leary, S. C., Cobine, P. A., Winge, D. R. & Chang, C. J. A targetable fluorescent sensor reveals that copper-deficient sco1 and SCO<sub>2</sub> patient cells prioritize mitochondrial copper homeostasis. *J. Am. Chem. Soc.* **133**, 8606–8616 (2011).
28. Er, J. C. et al. Neuo: a fluorescent chemical probe for live neuron labeling. *Angew. Chem. Int. Ed.* **54**, 2442–2446 (2015).
29. Que, E. L. et al. Quantitative mapping of zinc fluxes in the mammalian egg reveals the origin of fertilization-induced zinc sparks. *Nat. Chem.* **7**, 130–139 (2015).
30. Zhao, C. et al. Transforming the recognition site of 4-hydroxyaniline into 4-methoxyaniline grafted onto a BODIPY core switches the selective detection of peroxyxynitrite to hypochlorous acid. *Chem. Commun.* **52**, 2075–2078 (2016).
31. Zhang, Y. et al. 3-aminoBODIPY dyes: unexpected synthesis from 2-borate derivatives and application as fluorescent probe for alkaline pH range. *Tetrahedron Lett.* **57**, 4624–4628 (2016).
32. Liu, X.-L., Niu, L.-Y., Chen, Y.-Z., Yang, Y. & Yang, Q.-Z. A ratiometric fluorescent probe based on monochlorinated BODIPY for the discrimination of thiophenols over aliphatic thiols in water samples and in living cells. *Sens. Actuators B* **252**, 470–476 (2017).
33. Garwin, S. A. et al. Interrogating intracellular zinc chemistry with a long stokes shift zinc probe zincby-4. *J. Am. Chem. Soc.* **141**, 16696–16705 (2019).
34. Wang, Y. et al. Direct C-H amination of BODIPY core: synthesis and spectroscopic properties. *Dyes Pigm.* **177**, 108275 (2020).
35. Guisan-Ceinos, S. et al. Turn-on fluorescent biosensors for imaging hypoxia-like conditions in living cells. *J. Am. Chem. Soc.* **144**, 8185–8193 (2022).
36. Chen, L. et al. Red-emitting fluorogenic BODIPY-tetrazine probes for biological imaging. *Chem. Commun.* **58**, 298–301 (2022).
37. Wang, D. et al. Visible-light-induced direct photoamination of BODIPY dyes with aqueous ammonia. *Org. Lett.* **25**, 7650–7655 (2023).
38. Zhang, H. et al. Silver-mediated direct C-H amination of BODIPYs for screening endoplasmic reticulum-targeting reagents. *Chem. Commun.* **54**, 3219–3222 (2018).
39. Liu, J., Liu, J., Li, H., Bin, Z. & You, J. Boron-dipyrromethene-based fluorescent emitters enable high-performance narrowband red organic light-emitting diodes. *Angew. Chem. Int. Ed.* **62**, e202306471 (2023).
40. Lu, H., Mack, J., Nyokong, T., Kobayashi, N. & Shen, Z. Optically active BODIPYs. *Coord. Chem. Rev.* **318**, 1–15 (2016).
41. Pop, F., Zigon, N. & Avarvari, N. Main-group-based electro- and photoactive chiral materials. *Chem. Rev.* **119**, 8435–8478 (2019).
42. Abdou-Mohamed, A. et al. Stereoselective formation of boron-stereogenic organoboron derivatives. *Chem. Soc. Rev.* **52**, 4381–4391 (2023).
43. Li, X., Zhang, G. & Song, Q. Recent advances in the construction of tetracoordinate boron compounds. *Chem. Commun.* **59**, 3812–3820 (2023).
44. Braun, M. Boron-based enantiomerism. *Eur. J. Org. Chem.* **27**, e202400052 (2024).
45. Guo, Y., Zu, B., Du Chen, C. & He, C. Boron-stereogenic compounds: synthetic developments and opportunities. *Chin. J. Chem.* **42**, 2401–2411 (2024).
46. Imamoto, T. & Morishita, H. An enantiomerically pure tetra-coordinate boron compound: stereochemistry of substitution reactions at the chirogenic boron atom. *J. Am. Chem. Soc.* **122**, 6329–6330 (2000).
47. Kaiser, P. F., White, J. M. & Hutton, C. A. Enantioselective preparation of a stable boronate complex stereogenic only at boron. *J. Am. Chem. Soc.* **130**, 16450–16451 (2008).
48. Haefele, A., Zedde, C., Retailleau, P., Ulrich, G. & Ziessel, R. Boron asymmetry in a BODIPY derivative. *Org. Lett.* **12**, 1672–1675 (2010).
49. Gobo, Y., Matsuoka, R., Chiba, Y., Nakamura, T. & Nabeshima, T. Synthesis and chiroptical properties of phenanthrene-fused N<sub>2</sub>O-type BODIPYs. *Tetrahedron Lett.* **59**, 4149–4152 (2018).

50. Jimenez, V. G. et al. Circularly polarized luminescence of boronic acid-derived salicylidenehydrazone complexes containing chiral boron as stereogenic unit. *J. Org. Chem.* **83**, 14057–14062 (2018).
51. Ray, C. et al. Dissimilar-at-boron N-BODIPYs: from light-harvesting multichromophoric arrays to CPL-bright chiral-at-boron BODIPYs. *Org. Chem. Front.* **10**, 5834–5842 (2023).
52. Sanchez-Carnerero, E. M. et al. Unprecedented induced axial chirality in a molecular BODIPY dye: strongly bisignated electronic circular dichroism in the visible region. *Chem. Commun.* **49**, 11641–11643 (2013).
53. Ray, C. et al. Push-pull flexibly-bridged bis(haloBODIPYs): solvent and spacer switchable red emission. *Dalton Trans.* **45**, 11839–11848 (2016).
54. Gartzia-Rivero, L. et al. Chiral microneedles from an achiral bis(-boron dipyrromethene): spontaneous mirror symmetry breaking leading to a promising photoluminescent organic material. *Langmuir* **35**, 5021–5028 (2019).
55. Alnoman, R. B., Parveen, S., Hagar, M., Ahmed, H. A. & Knight, J. G. A new chiral boron-dipyrromethene (BODIPY)-based fluorescent probe: molecular docking, dft, antibacterial and antioxidant approaches. *J. Biomol. Struct. Dyn.* **38**, 5429–5442 (2020).
56. Zhao, L. et al. Biomimetic fluorescent probe for chiral glutamic acid in water and its application in living cell imaging. *Sens. Actuators B* **320**, 128383 (2020).
57. Zhang, G. et al. Cu(I)-catalyzed highly diastereo- and enantioselective constructions of boron/carbon vicinal stereogenic centers via insertion reaction. *ACS Catal.* **13**, 9502–9508 (2023).
58. Zhang, G. et al. Construction of boron-stereogenic compounds via enantioselective Cu-catalyzed desymmetric B-H bond insertion reaction. *Nat. Commun.* **13**, 2624 (2022).
59. Zu, B., Guo, Y. & He, C. Catalytic enantioselective construction of chiroptical boron-stereogenic compounds. *J. Am. Chem. Soc.* **143**, 16302–16310 (2021).
60. Zu, B., Guo, Y., Ren, L.-Q., Li, Y. & He, C. Catalytic enantioselective synthesis of boron-stereogenic BODIPYs. *Nat. Synth.* **2**, 564–571 (2023).
61. Lu, C.-J., Xu, Q., Feng, J. & Liu, R.-R. The asymmetric buchwald-hartwig amination reaction. *Angew. Chem. Int. Ed.* **62**, e202216863 (2023).
62. Zhou, F. et al. Copper-catalyzed desymmetric intramolecular ullmann C-N coupling: an enantioselective preparation of indolines. *J. Am. Chem. Soc.* **134**, 14326–14329 (2012).
63. Ramirez-Lopez, P. et al. Synthesis of IAN-type N,N-ligands via dynamic kinetic asymmetric buchwald-hartwig amination. *J. Am. Chem. Soc.* **138**, 12053–12056 (2016).
64. Kwon, Y., Chinn, A. J., Kim, B. & Miller, S. J. Divergent control of point and axial stereogenicity: catalytic enantioselective C-N bond-forming cross-coupling and catalyst-controlled atroposelective cyclodehydration. *Angew. Chem. Int. Ed.* **57**, 6251–6255 (2018).
65. Zhang, P. et al. Enantioselective synthesis of N-N bisindole atropisomers. *Angew. Chem. Int. Ed.* **61**, e202212101 (2022).
66. Wei, J., Gandon, V. & Zhu, Y. Amino acid-derived ionic chiral catalysts enable desymmetrizing cross-coupling to remote acyclic quaternary stereocenters. *J. Am. Chem. Soc.* **145**, 16796–16811 (2023).
67. Rohand, T., Baruah, M., Qin, W., Boens, N. & Dehaen, W. Functionalisation of fluorescent BODIPY dyes by nucleophilic substitution. *Chem. Commun.* 266–268 (2006).
68. Ripoll, C. et al. Synthesis and spectroscopy of benzylamine-substituted BODIPYs for bioimaging. *Eur. J. Org. Chem.* **2018**, 2561–2571 (2018).
69. Satoh, T., Fujii, K., Kimura, Y. & Matano, Y. Synthesis of 3,5-disubstituted BODIPYs bearing N-containing five-membered heteroaryl groups via nucleophilic C-N bond formation. *J. Org. Chem.* **83**, 5274–5281 (2018).
70. Qin, W. et al. 3,5-dianilino substituted difluoroboron dipyrromethene: Synthesis, spectroscopy, photophysics, crystal structure, electrochemistry, and quantum-chemical calculations. *J. Phys. Chem. C* **113**, 11731–11740 (2009).

## Acknowledgements

We are grateful for financial support from the National Natural Science Foundation of China (22122102, 22101120, 22271134, 22271313), Guangdong Provincial Key Laboratory of Catalysis (No. 2020B121201002), Guangdong Pearl River Talent Program (2019QN01Y628), and Shenzhen Science and Technology Innovation Commission (RCJC20221008092723013, JCYJ20230807093104009). We appreciate the assistance of SUSTech Core Research Facilities.

## Author contributions

C.H., B.Z., and L.Q.R. conceived the project. B.Z., L.Q.R., and J.Z. designed and performed the synthetic experiments. C.H. H.Z. and B.Z. prepared the manuscript. Correspondence should be sent to H.Z. (huazhang@scuec.edu.cn), C.H. (hec@sustech.edu.cn).

## Competing interests

The authors declare no competing interests.

## Additional information

**Supplementary information** The online version contains supplementary material available at <https://doi.org/10.1038/s41467-024-55796-5>.

**Correspondence** and requests for materials should be addressed to Hua Zhang or Chuan He.

**Peer review information** *Nature Communications* thanks Ying He, and the other, anonymous, reviewers for their contribution to the peer review of this work. A peer review file is available.

**Reprints and permissions information** is available at <http://www.nature.com/reprints>

**Publisher's note** Springer Nature remains neutral with regard to jurisdictional claims in published maps and institutional affiliations.

**Open Access** This article is licensed under a Creative Commons Attribution-NonCommercial-NoDerivatives 4.0 International License, which permits any non-commercial use, sharing, distribution and reproduction in any medium or format, as long as you give appropriate credit to the original author(s) and the source, provide a link to the Creative Commons licence, and indicate if you modified the licensed material. You do not have permission under this licence to share adapted material derived from this article or parts of it. The images or other third party material in this article are included in the article's Creative Commons licence, unless indicated otherwise in a credit line to the material. If material is not included in the article's Creative Commons licence and your intended use is not permitted by statutory regulation or exceeds the permitted use, you will need to obtain permission directly from the copyright holder. To view a copy of this licence, visit <http://creativecommons.org/licenses/by-nc-nd/4.0/>.

© The Author(s) 2025